Acetyl-11-keto-β-boswellic Acid Restrains Inflammation and Extracellular Matrix Degradation of Osteoarthritis via Suppression of NF-κB Pathway

Jing Zhou
Nanjing Medical University Affiliated Suzhou Hospital: Suzhou Municipal Hospital
https://orcid.org/0000-0003-2498-5273

Zeyu Han
Nanjing Medical University Affiliated Suzhou Hospital: Suzhou Municipal Hospital

Xueyan Li
Nanjing Medical University Affiliated Suzhou Hospital: Suzhou Municipal Hospital

Yinhua Qian
Nanjing Medical University Affiliated Suzhou Hospital: Suzhou Municipal Hospital

Lang Bai
Nanjing Medical University Affiliated Suzhou Hospital: Suzhou Municipal Hospital

Qibin Han
Nanjing Medical University Affiliated Suzhou Hospital: Suzhou Municipal Hospital

Xiaoyu Zhang
Nanjing Medical University Affiliated Suzhou Hospital: Suzhou Municipal Hospital

Qi Chen
Nanjing Medical University Affiliated Suzhou Hospital: Suzhou Municipal Hospital

Huaqiang Tao
First Affiliated Hospital of Soochow University

Maofeng Gao
First Affiliated Hospital of Soochow University

Yi Xue
Changshu Hospital Affiliated to Soochow University: First People's Hospital of Changshu City

Dan Hu
Nanjing Medical University Affiliated Suzhou Hospital: Suzhou Municipal Hospital

Dechun Geng
First Affiliated Hospital of Soochow University

Xing Yang (✉ xingyangsz@126.com)
Nanjing Medical University Affiliated Suzhou Hospital: Suzhou Municipal Hospital

Yuefeng Hao
Nanjing Medical University Affiliated Suzhou Hospital: Suzhou Municipal Hospital

Research Article

Keywords: acetyl-11-keto-β-boswellic acid, osteoarthritis, inflammation, extracellular matrix, NF-κB

Posted Date: January 18th, 2022

DOI: https://doi.org/10.21203/rs.3.rs-1234256/v1

Abstract

Background: Mechanical stress along with inflammation play causative roles in the development of osteoarthritis (OA), which decreases the quality of life and causes economic loss. Inflammation and extracellular matrix (ECM) degradation have been identified as key factors in the development of OA. As the main active component in frankincense, acetyl-11-keto-β-boswellic acid (AKBA) has been shown to have positive effects on inflammation. However, the effects of AKBA in cartilage inflammation and ECM degradation are currently elusive.

Methods: We demonstrated the role of inflammation and ECM degradation in the pathogenesis of OA and determined the protective effect of AKBA on both Hulth-Telhag rat OA model and lipopolysaccharide (LPS)-induced rat chondrocytes.

Results: We found increased inflammatory expression and decreased ECM expression in OA model cartilage and LPS-induced chondrocytes. Meanwhile, the protective effect of AKBA and its inhibitory effects on inflammation as well as ECM-related markers were also observed in the rat Hulth-Telhag model. Furthermore, activation of NF-κB attenuated nuclear p65 protein levels in chondrocytes upon LPS stimulation. In addition, AKBA was found to subsequently reversed the LPS-induced activation of NF- κB signal and inflammation-related ECM degradation in chondrocytes.

Conclusions: Suppression of NF-κB pathway activation by AKBA restrains OA development via inhibition of inflammation and ECM degradation. AKBA is a promising therapeutic agent for the treatment of OA.

1 Background

Osteoarthritis (OA), a quite common chronic and degenerative disease in orthopedics, decreases the quality of life and causes economic loss globally.(1) The incidence of OA is continuously increasing because of aging, genetic factors, inflammation, obesity, and biological and biomechanical factors.(2, 3) The development of OA cannot be reversed and terminated under current technical conditions. The specific principle is non-drug therapy combined with medication palliative treatment is mainly applied to relieve symptoms, if necessary, surgical treatment.(4) However, high cost, prosthesis loosening, secondary revision of wear, unnatural angle of movement, and limited movement limit the surgical treatment. Currently, there are various drugs used to treat OA, of which nonsteroidal anti-inflammatory drugs (NSAIDs) are the most widely used. However, long-term use of NSAIDs can confer negative effects on coagulation, digestion, and urinary systems.(5) Therefore, exploring the pathogenesis and treatment of OA could be of great practical significance.

Biological and biomechanical factors such as mechanical stress and inflammation disrupt the balance between anabolism and catabolism of chondrocytes, extracellular matrix (ECM), and subchondral bone, leading to degenerative fibrosis of joint cartilage and subchondral bone sclerosis.(4, 6) Inflammation and ECM degradation represent hallmarks of OA progression, resulting in the pathological changes of OA. Elevated inflammatory factors, such as interleukin (IL)-1β, IL-6, and tumor necrosis factor (TNF)-α, can

promote the expression of matrix metalloproteinases (MMPs) and other catabolic enzymes to destruct the ECM, which have been reported to upset the balance between anabolism and catabolism in normal cartilage.(7-9) As essential components of the ECM, the expression level of aggrecan and collagen II (col II) is an important indicator of the degree of cartilage degeneration and its decreased activity can lead to ECM regeneration disorder, eventually causing cartilage degeneration.(10)

Frankincense, the resin exuded from the bark of *Boswellia carterii* birdw, which belongs to Oleaceae plants, has long been recognized as a traditional medicine in India and China.(11) Studies have found that acetyl-11-keto-β-boswellic acid (AKBA) can significantly alleviate the symptoms of OA.(12) As the most active ingredient in frankincense, AKBA has become the primary research object with stronger biological activity than 11-keto-β-boswellic acid (KBA).(13, 14) Multiple studies have found that AKBA has anti-inflammatory, analgesic, anti-ulcer, anti-oxidation, anti-tumor, anti-osteogenic inhibition, immunomodulatory, and lipid regulatory capabilities.(15-19) Whereas few studies have associated AKBA with cartilage metabolism, others have indicated that AKBA could relieve the symptoms of OA. Moreover, the specific mechanism of AKBA on the development of OA has not been investigated, which restricts the further application of AKBA and its derivatives.

Herein, we probed the association between AKBA intervention and surgery and lipopolysaccharide (LPS)-induced inflammation and ECM degradation. Hulth-Telhag OA model was used *in vivo* and LPS was used to induce inflammation *in vitro*. Our results confirmed that AKBA intervention attenuated inflammation and ECM degradation. The inhibition of inflammation and ECM degradation was achieved through AKBA-mediated inhibition of the NF-κB signaling pathway. In a nutshell, these results demonstrate that AKBA is a promising therapeutic approach for the prevention and treatment of OA.

2 Materials And Methods

2.1 Ethics statement

Animal welfare and experimental procedures were carried out in accordance with the Declaration of Helsinke, and were approved by the Ethics Committee of the First Affiliated Hospital of Soochow University.

2.2 Compounds and reagents

AKBA (CAS No.: 67416-61-9, purity: 99.71%) was purchased from MCE (Shanghai, China). N-3-oxo-dodecanoyl-L-Homoserine lactone (3-O-C12-HSL, Cas No.:168982-69-2, purity: 98.00%) was purchased from Apexbio (Houston, USA).

2.3 Animals and experimental design *in vivo*

Approximately 24 eight-week-old Sprague Dawley (SD) male rats were raised in a standard environment and were randomly kept in cages, where water and fodder supply were sufficient. The Hulth-Telhag OA model was established. After one week of adaption feeding, SD rats were randomly divided into four

groups: control, vehicle, low-AKBA, and high-AKBA groups (n = 6/group). Except for the control group, the rats in the other three groups received chloral hydrate (1 mg/kg, intraperitoneally) for anesthesia. After anesthesia, both lower extremity operation area of the rat was shaved, followed by repeated penicillin G (80000 U/rat) intramuscular administration for 3 days. The operation area was disinfected per the aseptic operation regulations, the anterior medial longitudinal skin incision was taken, the knee joint was exposed, and the medial side was cut off. The medial collateral ligament, the anterior and posterior cruciate ligaments, and the medial meniscus were removed. The articular cartilage surface was protected during the operation. The joint cavity and epidermis were sutured layer by layer using a 3-0 silk thread. The affected limb was not fixed after the operation. The experimental animals were returned to the animal room to continue feeding. One week after modelling, the rats were administered with 0.5 ml/kg saline, as well as 2 and 8 mg/kg AKBA solution by gavage every other day. All experimental animals were sacrificed after 6 weeks and samples were taken for analysis.

2.4 Micro-computed tomography (micro-CT) and reconstruction

The rats were sacrificed after 6 weeks by intraperitoneal injection of excess pentobarbital sodium, and the knee joint (n = 6/group) were collected and fixed with 10% paraformaldehyde. A SkyScan 1176 CT machine (BRUKER, Belgium) was used for CT. The scanning parameters were 60 kV source voltage and 170 μA source current, and the resolution was set at 9 μm. The 3D reconstruction used the procedure provided by the factory. Bone trabecular bone density (Tb. BMD, mg/cm^3), bone volume fraction (BV/TV, %), number of trabecular bone (Tb. N, mm^{-1}), the thickness of trabecular bone (Tb. Th, μm), trabecular bone separation (Tb. Sp, mm), and connection density (Conn. D, mm^{-1}) were analyzed with SkyScan software.

2.5 Histologic analysis

For decalcification, samples from each group were placed into 10% ethylenediaminetetraacetic acid (EDTA) for 4 weeks, paraffin-embedded samples were cut into 6-μm slices and staining procedures, including hematoxylin and eosin (H&E), safranin O-fast green, and tartrate-resistant acid phosphatase (TRAP) staining, were performed according to the manufacturer's protocols. An AxioCam HRc microscope (Carl Zeiss, Jena, Germany) was used to capture the images. Morphological scores of H&E and safranin O-fast green staining were given to sections under a micro-imaging system according to the International Academy of Osteoarthritis Research (OARSI) scores, and three readers were arranged for each section to obtain the average as the final score. After TRAP staining was completed, 5 fields of vision under the cartilage or above the tide line were randomly selected, the number of TRAP-positive cells, and the proportion of osteoclast surface (OcS/BS, %) were counted using the BIOQUANT OSTEO (BIOQUANT, USA).

2.6 Immunohistochemical (IHC) analysis

Expression levels of IL-1β, IL-6, TNF-α, MMP13, col Ⅱ, col Ⅹ, IKKα/β, IκBα, and p65 in the knee joint was examined using IHC analysis with corresponding primary antibodies (Abcam, ab9722, ab9324, ab9739, ab39012, ab34712, ab39012, ab178870, ab32518, and ab16502). Briefly, the sections were dewaxed for 1 h with xylene and then subjected to gradient hydration, antigen retrieval with hyaluronidase (1 h, 37°C), and pepsin (25 min, RT). Next, the sample sections were blocked with bovine serum albumin (BSA, 1 h, room temperature (RT)), followed by incubation with correspondent primary antibodies (12 h, 4°C). After washing with PBS, sections were incubated with secondary antibodies (30 min, RT). The chromogenic reaction was induced by a DAB horseradish peroxidase color development kit (Beyotime, Shanghai, China). In the semi-quantitative analysis, positive cell counts were randomly selected under the microscope to count positive cells and non-positive cells, and the proportion of positive cells was obtained. The average number was used as the proportion of positive cells in the section. The average optical density analysis was completed with Image Pro-Plus 6.0 software, and uniform white balance and exposure time settings used in the screenshot were adopted. Because col II is only concentrated on the surface of the cartilage, the only semi-quantitative analysis was performed on the surface of the cartilage.

2.7 Cell culture

Rat primary articular chondrocytes (Cat NO.: CP-R092) was purchased from Procell (Wuhan, China). After digestion by 0.25% trypsin, chondrocytes were cultured in F-12 medium mixed with 10% fetal bovine serum (FBS) and 1% penicillin/streptomycin in a regular incubator (37°C, 5% CO_2). The medium was changed every 3 days. Cells subculturing was performed when the cells reached 80-90% confluency after washing and digestion. Cells were then treated with AKBA in low (2 μM) or high (8 μM) concentrations.

2.8 Cell viability assay

Chondrocytes were seeded (5×10^3/well in 0.5 ml of F-12 medium) in 96-well plates and cultured with a range of concentrations of AKBA (0, 2, 4, 8, 16, 32, 64, and 128 μM) for 24, 48, and 72 h after adherence. After reaching the corresponding time point, the PBS-washed cells were incubated with a cell counting kit-8 (CCK-8) (Dojindo, Shanghai, China) (3h, 37°C) and the optical density (OD) of chondrocytes at 450 nm was determined. The cell viability to control was calculated using the equation: Cell viability to control (%) = OD drug-treated group/OD control group.

2.9 Western blot analysis

After treatment, cell proteins were extracted using radioimmunoprecipitation assay (RIPA) buffer with protease inhibitors and phosphatase inhibitors. The protein concentration was determined by a nucleic acid-protein quantometer (Thermo Scientific, Shanghai, China), and then separated by sodium dodecyl sulfate-polyacrylamide gel electrophoresis (SDS-PAGE). The resolved proteins were transferred to a polyvinylidene difluoride (PVDF) membrane and blocked with blocking solution (1 h, RT). Next, PVDF membranes were incubated with corresponding primary antibodies (overnight, 4°C), followed by incubation with the secondary antibody (1 h, 4°C). The reactive protein bands were detected by the Western blot detection kit. Image analysis was performed using Image J software.

2.10 Quantitative real-time (qRT)-PCR

After treatment, total RNA was extracted using Beyozol reagent (Beyotime, Shanghai, China). The quality of RNA was confirmed by measuring the absorbance of the A260/A280 and A260/A230 ratio in the range of 1.8-2.0, respectively. cDNA was synthesized with MonScript™ RTIII Super Mix with dsDNase (Monad, Wuhan, China) following the manufacturer's protocols. Subsequently, MonAmp™ ChemoHS qPCR Mix (Monad, Wuhan, China) was used to perform qRT-PCR. The parameters were as follows: 95.0°C for 10 min, 40 cycles of 95.0°C for 10 s, 60.0°C for 10 s, and 72.0°C for 10 s. All samples were analyzed in triplicate and three independent experiments. The comparative $2^{-\Delta\Delta Cq}$ method was used for analysis. GraphPad Prism 8 software was used to perform statistical analysis and draw graphs. The primer sequences are shown in Table 1.

2.11 Immunofluorescence (IF) assay

Chondrocytes climbing slices were incubated with or without LPS (1 μg/ml) for 24 h, and then co-incubated with or without AKBA (1 μM) for 24 h. PBS-washed slices were fixed in 4% paraformaldehyde solution (15 min, RT), washed thrice with PBS, and then treated with 0.1% TritonX-100 (5 min, RT). Climbing slices were then shifted into a wet box, blocked with blocking solution (1 h, 37°C), and then incubated with primary antibodies (MMP13 (1:200) and p-p65 (1: 200)) diluted with their dilutions for 12 h at 4°C. After incubating with iFluor™ 488 goat anti-rabbit IgG antibody (1:1000, AAT Bioquest, Calif, USA) in darkness for 1 h, DAPI (4',6-diamidino-2-phenylindole) was used to stain the cell nuclei. The slices were dried and sealed by an anti-fluorescence quenching agent and imaged using confocal microscopy (Carl Zeiss AG, Jena, Germany) after aspirating the liquid from the climbing slices.

2.12 Statistical analysis

The quantitative data were expressed as the means ± standard deviation (SD). GraphPad Prism 8 (GraphPad Software Inc, USA) was utilized for data analysis and statistical mapping. The two samples were compared using an independent sample t-test. A P-value <0.05 was considered statistically significant.

3 Results

3.1 AKBA treatment had positive effects on the development of a surgery-induced OA rat

To explore the potential effects of AKBA in the development of OA, a Hulth-Telhag model was established (Fig. S1). AKBA was administered for 6 weeks intraperitoneally after the operation. Micro-CT, H&E staining, safranin O-fast green staining, TRAP staining, and OARSI scores were used to observe the

cartilage structure, the morphological appearance of the cartilage cells, and osteoclast activity difference in the control, vehicle, and low/high-AKBA groups. Micro-CT analysis indicated that specimens in the controls had a normal joint space and bone mineral density. The vehicle group had narrowing of the joint space and hyper osteogeny; however, in the AKBA-treatment group, these were reversed (Fig. 1(A)). Bone morphometric analysis was performed to further quantify and compare the parameters of the trabecula. The results showed that several parameters of the bone trabecula, such as BV/TV, Tb. N, Tb. Th, Conn. D, etc., decreased in the solvent group compared to the controls while Tb. Sp increased and the difference was significant (Fig. 1(B)-(G)). After AKBA treatment, the decrease of BV/TV, Tb. N, and Conn. D decreased and the increase of Tb. Sp decreased in the low-AKBA group. Collectively, these statistics showed that AKBA eased surgery-induced changes in the subchondral bone.

After treatment, specimens were counterstained with H&E and safranin O-fast green staining (Fig. 1(H)). Sections were examined under a microscope based on the OARSI scoring system (Fig. 1(I)-(K)). The control group grade averaged 0.1667, with a staged interval of 0-1.0, the cartilage surface was intact, and the cell structure was normal. The solvent group grade averaged 3.750, with a staged interval of 2.5-4.5, with marked cartilage matrix loss. Large cysts were formed in the area, chondrocytes clustered, some cells were significantly enlarged, cartilage structure was disordered, and degeneration was substantial. In the low-AKBA group, the average grade was 2.750 and the stage interval was 2.0-3.5. There was a phenomenon of focal deep staining. Occasionally, cracks penetrated deep into the cartilage area, and there was chondrocytes clustering and hypertrophy. The high-AKBA group had an average grade of 1.5 and a stage interval of 1.0-2.0. The surface of the cartilage was discontinuous and there was focal staining. It was enhanced, but cell hypertrophy and clustering phenomenon was not evident, and the degree of degeneration was lighter. The solvent composition level was significantly different from the controls ($P<0.01$). The improvement of the solvent composition level was significant ($P<0.05$) and the difference between the low-AKBA and the high-AKBA groups was also significant ($P<0.01$). It showed that AKBA could alleviate the depth of arthritis invading cartilage. In terms of staging, there was a significant difference between the vehicle group and the control group ($P<0.01$) but there was no significant difference in staging between the low-AKBA group and the high-AKBA. Because the stage mainly shows the size of the affected area of the joint, the effect of AKBA on the size of the affected area was relatively small. In terms of the overall score, the vehicle group was also significantly different from the controls (P<

Next, we performed TRAP staining on the specimens to identify differences in osteoclast activity between different groups. The results showed that the osteoclast was more active in the vehicle group than in the controls (Fig. S2(A)), which is consistent with the findings of micro-CT. About the quantitative analysis, the vehicle group increased significantly compared to the control group (Fig. S2(B) and (C)) both in the TRAP-positive cell count and OcS/BS, suggesting that the osteoclast was very active in the early stage of OA. In the AKBA intervention group, the osteoclast count in the low-AKBA group decreased compared with OcS/BS in the vehicle group, which were 44.9% ($P<0.05$) and 32.0% ($P<0.05$), respectively, and the difference was significant. Interestingly, this effect was also evident in the high-AKBA group, reaching 67.6% ($P<0.01$) and 77.9% ($P<0.01$). However, between the low-AKBA and the high-AKBA groups, the

TRAP-positive cell count did not show a significant difference, but there were significant differences in OcS/BS, showing a dose-dependent effect (Fig. S2(B) and (C)).

3.2 AKBA treatment repressed inflammation and ECM degradation in surgery-induced OA rat

To delve deeper into whether AKBA treatment could attenuate inflammation and ECM degradation in surgery-induced OA rats, specimens were immunoassayed to evaluate the expression of inflammatory and ECM biomarkers. AKBA intervention significantly eased the expression levels of inflammatory markers in surgery-induced OA rats (Fig. 2(A)). However, more IHC-positive cells were observed in the vehicle group compared with the other groups. These results implied that the removal of the medial collateral ligament, the anterior and posterior cruciate ligaments, and the medial meniscus enhanced the expression of inflammatory markers, while AKBA intervention reversed the results (Fig. 2(B)-(D)).

We selected common cartilage degeneration markers MMP13 and major cartilage matrix components col and (Fig. 2(E)) for IHC, of which MMP13 was closely related to cartilage degeneration and its expression level was strongly associated with the level of cartilage degeneration. The IHC analysis showed that the average proportion of MMP13-positive cells in the vehicle group increased by nearly 1.5 times compared with the controls, and the degeneration performance was significant. The proportion of positive cells in the vehicle group was higher than that in the high-AKBA group at the same time. The average values decreased by 35.9% and 53.4%, respectively, and the difference was significant ($P<0.01$). Similarly, the difference between the high-AKBA group and the low-AKBA group was also significant. We noticed that in the control group, col II was mainly concentrated on the surface of cartilage, where there was almost no col I. Col I content, however, was higher below the surface layer. In the vehicle group, we found that col II staining depth of the cartilage surface layer decreased significantly and more col I appeared, suggesting severe matrix loss and active fibrogenesis. In the AKBA treatment groups, the staining depth of col I increased, while the staining depth of col I on the surface of cartilage decreased (Fig. 2(E)). Semi-quantitative analysis (Fig. 2(G)-(J)) showed that col II-positive cells and expression decreased in the state of arthritis, while the expression of col I and the number of positive cells increased. However, col expression increased whereas col expression AKBA treatment alleviated LPS-induced inflammation and ECM degradation in chondrocytes

The chemical structure of AKBA and 3-O-C12-HSL were showed in Fig. S3(A) and (D). To determine the cytotoxicity of AKBA and 3-O-C12-HSL on rat chondrocytes, chondrocytes were cultured in a series of concentrations (0, 1, 2, 4, 8, 16, 32, 64, and 128 μM) of AKBA for 1, 2, and 3 days separately, before cell viability was detected by CCK-8 assay. The results indicated that AKBA and 3-O-C12-HSL affected the viability of chondrocytes when the concentration was >8 μM (Fig. S3(B) and (C)) and >16 μM (Fig. S3(E) and (F)) on the third day. This shows that AKBA at 2 and 8 μM can be utilized in the subsequent experiments.

The mixed chondrocytes were pretreated by 1 μg/ml LPS for 24 h followed by treatment with low (2 μM) or high (8 μM) concentrations of AKBA for 24 h to evaluate the potential inflammatory effects of AKBA in

LPS-induced chondrocytes. Western blotting and qRT-PCR were used to test the protein and mRNA levels of inflammatory biomarkers. Although LPS-stimulated production of IL-1β, IL-6, and TNF-α was significantly upregulated compared with the controls, these biomarkers were reversed by AKBA at 2 μM and 8 μM in a dose-dependent trend (Fig. 3(A)-(D)). Meanwhile, there was significant downregulation of inflammatory mRNA levels (Fig. 3(E)-(G)). The results indicated that AKBA could suppress the LPS-induced inflammatory response in chondrocytes in a concentration-dependent manner.

IF analysis was performed to visualize infected cells, which significantly reversed the downregulation of col II (Fig. 3H). We investigated the effects of AKBA on aggrecan, col II, and MMPs mRNA and protein expression to confirm whether AKBA could protect against LPS-induced matrix degradation. The results showed that AKBA enhanced aggrecan and col II protein (Fig. 3(I)-(K)) and mRNA (Fig. 3(O) and (P)) expression in LPS-induced chondrocytes, which was dependent on AKBA concentration. As expected, the expression levels of MMP1, MMP3, and MMP13, which are strongly related to OA development, increased in LPS-stimulated chondrocytes. However, AKBA treatment significantly reversed the LPS-induced upregulation of MMPs at protein (Fig. 3(I), (L)-(M)) and mRNA (Fig. 3(Q)-(S)) levels.

Overall, these results demonstrated that AKBA could efficiently reverse ECM and maintain the phenotype in LPS-induced rat articular chondrocytes.

3.3 AKBA treatment inhibited NF-κB activation *in vitro* and *in vivo*

We detected the expression of pivotal markers involved in related signaling pathways to examine the underlying molecular mechanisms of AKBA intervention. IHC staining of p65, IKKα, and IκBα was performed to confirm that AKBA treatment could suppress surgery-induced inflammation and ECM degradation via NF-κB signaling pathway in rat knees. There was a high expression of p65 and IKKα in the model group and intense IκBα staining in AKBA-treated rats, compared with the low expression observed in vehicle rats (Fig. 4(A)). Semi-quantitative analysis indicated that compared with controls, the removal of ligaments and meniscus increased the expression of p65 and IKKα but reduced IκBα expression, respectively (Fig. 4(B)-(D)). AKBA intervention corrected the effects of surgical stimulation. These data showed that AKBA alleviated surgery-induced inflammation and ECM degradation via suppression of the NF-κB signaling pathway *in vivo*.

Among the three classic IκB proteins, IκBα is the strongest negative feedback factor in the activation of NF-κB, which ensures the rapid occurrence and shutdown of NF-κB activation. The classical NF-κB signaling pathway was activated and IκBα was rapidly degraded upon LPS induction (Fig. 5(A)-(C)). Interestingly, after AKBA treatment, the degradation of IκBα was restored. Western blot and qRT-PCR analyses demonstrated that LPS activated the levels of p65. However, the p65 level was markedly decreased in AKBA-treated chondrocytes compared to LPS-treated cells only. Western blot analysis of p-IKKα/β, IKKα, IKKβ, p-p65, p65, p-IκBα, and IκBα showed that AKBA intervention affected the ratio of p-IKKα/β to IKKα plus IKKβ, p-p65 to p65 and p-IκBα to IκBα induced by LPS, respectively. These results showed that the protective effects of AKBA may be mediated by repressing the NF-κB signaling pathway.

3-O-C12-HSL is an acyl-homoserine lactone (AHL), an activator of NF-κB. We first confirmed that 3-O-C12-HSL could promote inflammation and ECM degradation. Western blotting (Fig. S4) showed a drastic increase in the expression of inflammatory factors and MMPs after 3-O-C12-HSL treatment. As expected, the expression of aggrecan and collagen II were drastically inhibited in 3-O-C12-HSL-treated chondrocytes compared to controls (Fig. S4(B), (F), and(G)). Moreover, we observed the effects of 3-O-C12-HSL on AKBA-treated chondrocytes. Medicare, 5 μM of 3-O-C12-HSL elevated levels of inflammatory factors and MMPs, and decreased protein and mRNA levels of aggrecan and collagen II at the same time(Fig. S5).

Strikingly, treatment with 5 μM of 3-O-C12-HSL (contained 1 μg/ml LPS and 8 μM AKBA) reversed the AKBA-mediated rescue of the LPS-induced activation of the NF-kB signaling pathway. The results indicated that 3-O-C12-HSL activated protein expression of p65 and IκBα (Fig. S6(A)-(C)). IF analysis also indicated that AKBA intervention promoted the inhibition of p65 and decreased its nuclear translocation (Fig. S6(D)). Nevertheless, these effects were suppressed after the intervention of 3-O-C12-HSL (Fig. S6(F)). Overall, 3-O-C12-HSL severely inhibited the protective effect of AKBA on NF-κB inhibition. These findings denoted that AKBA intervention resolved the activation of the LPS-induced NF-κB signaling pathway, while 3-O-C12-HSL treatment reversed the positive effect of AKBA in LPS-induced inflammation and ECM degradation.

4 Discussion

Mounting studies have identified that a combination of biological and mechanical factors disrupts the synthesis and degradation balance of chondrocytes, ECM, and subchondral bone, causing cartilage degeneration, fibrosis, and subchondral callus.(6, 8, 9, 20, 21) Mechanical stimulation leads to metabolic changes, which are characterized by the release of inflammatory mediators and MMPs and the degradation of ECM.(7, 22-24) Under normal circumstances, anabolism and catabolism of ECM are in a dynamic equilibrium, which is essential for a healthy joint.(24) Once the balance is disrupted, it leads to irreparable joint cartilage damage and OA symptoms. Alleviating the inflammatory mediators and ECM degradation is a key player in the prevention versus treatment of OA. Despite some breakthroughs made in illuminating the pathogenesis of OA, there are no disease-modifying drugs with evidently validated therapeutic effects to modify the progression of OA at present.(4, 5, 8)

Natural products could treat various human diseases, including OA, after their widespread use, half of which are likely extracted from plants.(25-29) AKBA, a pharmacologically active pentacyclic triterpenes compound from *Boswellia serrate* extract, has been reported previously to alleviate host inflammatory response, mitigating inflammation-induced damage to diabetes, bronchial and nervous tissue.(15, 30-32) In addition, it has been reported that AKBA has anti-osteogenic inhibition, anti-ulcer, anti-asthma, anti-oxidative stress, anti-tumor, and lipid regulatory effects.(16-18) AKBA inhibited inflammation through NF-κB-regulated gene expression. We concluded that AKBA reversed the imbalance of LPS-induced inflammation and ECM metabolism by inhibiting the NF-κB pathway. Additionally, we demonstrated that AKBA intervention alleviated the progress of OA in a rat Hulth-Telhag OA model for the first time.

Several studies have reported that the NF-κB signaling pathway plays an important role in the pathophysiological process of OA and is activated by the inflammation of OA, as such, the upstream regulators, co-factors, and downstream effectors of NF-κB have become promising targets of OA and rheumatoid arthritis therapies.(33-35) Based on current studies, NF-κB plays a vital part in inducing various inflammatory-related factors, including IL-1β, IL-6, TNF-α, and MMP proteins, which can stimulate chondrocyte catabolism.(36-38) NF-κB is also related to ECM degradation. As the two most abundant components in the ECM, aggrecan and col II are degraded by MMPs, whose increased expression is regulated by NF-κB.(39, 40) Furthermore, NF-κB can phosphorylate and degrade IκB protein when chondrocytes are stimulated by various stimuli, causing the transport of NF-κB p65 to the nucleus, where p65 facilitates OA-related gene and protein expression. Our study suggested that AKBA treatment inhibited the overexpression of IL-1β, IL-6, and TNF-α using Western blot and qRT-PCR. Further, AKBA treatment reversed the degradation of aggrecan and col II and the upregulation of MMPs. The results also suggested that AKBA treatment could inhibit nuclear translocation of p-p65 by Western blot and IF analyses. Taken together, these results showed that AKBA treatment plays a positive role in anti-inflammation and ECM degradation by inactivating the NF-κB signaling pathway (Fig. 6).

3-O-C12-HSL, one of the AHLs frequently identified in extracts of respiratory secretions from cystic fibrosis patients infected with *Pseudomonas aeruginosa* and *Burkholderia cepacia* complex species and acts as an activator of NF-kB, was used to verify the role of the NF-kB pathway.(41-43) IF assay indicated that AKBA treatment depressed nuclear translocation of p65 after LPS-induced cytoplasmic localization. However, 3-O-C12-HSL treatment reversed the effects of AKBA on the inhibition of p65 in chondrocytes. Overall, our results demonstrated that AKBA intervention restrained LPS-induced inflammation and ECM degradation via suppression of the NF-κB signaling pathway.

5 Conclusion

In this integrative study, we found that AKBA alleviated inflammation and ECM degradation, which may be related to the regulation of NF-κB. However, the effects of other related signaling pathways have not been ruled out and should be investigated in subsequent experiments. Besides, we found that osteoclast was more active in the vehicle group than in controls, which was consistent with micro-CT findings. These results suggest that AKBA may be a potential drug target to prevent and treat OA by enhancing anti-inflammatory and inhibiting ECM degradation.

6 Abbreviations

OA: osteoarthritis; AKBA: acetyl-11-keto-β-boswellic acid; KBA: 11-keto-β-boswellic acid; MMP: matrix metalloproteinase; ECM: extracellular matrix; SD: Sprague Dawley; Tb. BMD: Bone trabecular bone density; BV/TV: bone volume fraction; Tb. N: number of trabecular bone; Tb. Th: thickness of trabecular bone; Tb. Sp: trabecular bone separation; Conn. D: connection density; H&E: hematoxylin and eosin; IHC: immunohistochemistry; IF: immunofluorescence; OcS/BS: the proportion of osteoclast surface; LPS: lipopolysaccharide; NF-κB: nuclear factor kappa B; NSAIDs: nonsteroidal anti-inflammatory drugs; IL:

interleukin; TNF: tumor necrosis factor; TRAP: tartrate-resistant acid phosphatase; OARSI: International Academy of Osteoarthritis Research; RT: room temperature; FBS: fetal bovine serum; PBS: phosphate buffer saline; CCK-8: cell counting Kit-8; RIPA: radioimmunoprecipitation assay; PVDF: polyvinylidene difluoride; qRT-PCR: quantitative real-time PCR; DAPI:2-(4-Amidinophenyl)-6-indolecarbamidine dihydrochloride.

7 Declarations

Ethics approval and consent to participate

Animal welfare and experimental procedures were carried out in accordance with the Declaration of Helsinke, and were approved by the Ethics Committee of the First Affiliated Hospital of Soochow University.

Consent for publication

We declare that the Publisher has the Author's permission to publish the relevant contribution.

Availability of data and materials

Not applicable.

Competing interests

The authors declare no competing confct of interests.

Fundings

Financial supports from National Natural Science Foundation of China (No. 82072425, 81873991 and 81672238); Natural Science Foundation of Jiangsu Province (No. BK20180001 and BK20211083); Jiangsu Commission of Health (No. H2018027); Jiangsu social development project (No. BE2021673); Graduate Research and Practice innovation Plan of Graduate Education Innovation Project in Jiangsu Province (KYCX21_1578); Suzhou Jiangsu Commission of Health (No. SYS2019100 and SYS2019101), Suzhou Health Committee gusu Health Personnel Training project (GSWS2020078); Project of Suzhou Sports Research Bureau (No. TY2019-204), and Special Project of Diagnosis and Treatment Technology for Key Clinical Diseases in Suzhou (LCZX202003).

Authors' contributions

Jing Zhou: writing – review & editing, data curation, methodology. **Zeyu Han Shao**: data curation, methodology. **Xueyan Li**: data curation, methodology. **Yinhua Qian**: data curation, methodology. **Lang Bai**: data curation, software. **Qibin Han:** investigation, validation. **Xiaoyu Zhang**: investigation, validation. **Qi Chen:** methodology. **Huaqiang Tao**: formal analysis, methodology. **Maofeng Gao**: formal analysis, methodology. **Yi Xue**: formal analysis, methodology. **Dan Hu**: resources. **Dechun Geng**: funding

acquisition, resources. **Xing Yang**: supervision, project administration. **Yuefeng Hao**: conceptualization, supervision.

Acknowledgements

We would like to thank the Institute of Orthopedics, Soochow University limited for their technical support.

8 References

1. Glyn-Jones S, Palmer AJR, Agricola R, Price AJ, Vincent TL, Weinans H, et al. Osteoarthritis. The Lancet. 2015;386(9991):376-87.
2. Reyes C, Leyland KM, Peat G, Cooper C, Arden NK, Prieto-Alhambra D. Association Between Overweight and Obesity and Risk of Clinically Diagnosed Knee, Hip, and Hand Osteoarthritis: A Population-Based Cohort Study. Arthritis Rheumatol. 2016;68(8):1869-75.
3. Loeser RF, Collins JA, Diekman BO. Ageing and the pathogenesis of osteoarthritis. Nat Rev Rheumatol. 2016;12(7):412-20.
4. Mandl LA. Osteoarthritis year in review 2018: clinical. Osteoarthritis Cartilage. 2019;27(3):359-64.
5. Zeng C, Wei J, Persson MSM, Sarmanova A, Doherty M, Xie D, et al. Relative efficacy and safety of topical non-steroidal anti-inflammatory drugs for osteoarthritis: a systematic review and network meta-analysis of randomised controlled trials and observational studies. Br J Sports Med. 2018;52(10):642-50.
6. Xia B, Di C, Zhang J, Hu S, Jin H, Tong P. Osteoarthritis pathogenesis: a review of molecular mechanisms. Calcif Tissue Int. 2014;95(6):495-505.
7. Mehana EE, Khafaga AF, El-Blehi SS. The role of matrix metalloproteinases in osteoarthritis pathogenesis: An updated review. Life Sci. 2019;234:116786.
8. Lieberthal J, Sambamurthy N, Scanzello CR. Inflammation in joint injury and post-traumatic osteoarthritis. Osteoarthritis Cartilage. 2015;23(11):1825-34.
9. Carballo CB, Nakagawa Y, Sekiya I, Rodeo SA. Basic Science of Articular Cartilage. Clin Sports Med. 2017;36(3):413-25.
10. Mobasheri A, Bay-Jensen AC, van Spil WE, Larkin J, Levesque MC. Osteoarthritis Year in Review 2016: biomarkers (biochemical markers). Osteoarthritis Cartilage. 2017;25(2):199-208.
11. Ning Z, Wang C, Liu Y, Song Z, Ma X, Liang D, et al. Integrating Strategies of Herbal Metabolomics, Network Pharmacology, and Experiment Validation to Investigate Frankincense Processing Effects. Front Pharmacol. 2018;9:1482.
12. Sengupta K, Alluri KV, Satish AR, Mishra S, Golakoti T, Sarma KV, et al. A double blind, randomized, placebo controlled study of the efficacy and safety of 5-Loxin for treatment of osteoarthritis of the knee. Arthritis Res Ther. 2008;10(4):R85.
13. Roy NK, Parama D, Banik K, Bordoloi D, Devi AK, Thakur KK, et al. An Update on Pharmacological Potential of Boswellic Acids against Chronic Diseases. Int J Mol Sci. 2019;20(17).

14. Miscioscia E, Shmalberg J, Scott KC. Measurement of 3-acetyl-11-keto-beta-boswellic acid and 11-keto-beta-boswellic acid in Boswellia serrata Supplements Administered to Dogs. BMC Vet Res. 2019;15(1):270.
15. Meka B, Ravada SR, Murali Krishna Kumar M, Purna Nagasree K, Golakoti T. Synthesis of new analogs of AKBA and evaluation of their anti-inflammatory activities. Bioorg Med Chem. 2017;25(4):1374-88.
16. Tambe A, Mokashi P, Pandita N. Ex-vivo intestinal absorption study of boswellic acid, cyclodextrin complexes and poloxamer solid dispersions using everted gut sac technique. J Pharm Biomed Anal. 2019;167:66-73.
17. Rajabian A, Sadeghnia HR, Hosseini A, Mousavi SH, Boroushaki MT. 3-Acetyl-11-keto-beta-boswellic acid attenuated oxidative glutamate toxicity in neuron-like cell lines by apoptosis inhibition. J Cell Biochem. 2020;121(2):1778-89.
18. Li W, Liu J, Fu W, Zheng X, Ren L, Liu S, et al. 3-O-acetyl-11-keto-beta-boswellic acid exerts anti-tumor effects in glioblastoma by arresting cell cycle at G2/M phase. J Exp Clin Cancer Res. 2018;37(1):132.
19. Xiong L, Liu Y, Zhu F, Lin J, Wen D, Wang Z, et al. Acetyl-11-keto-beta-boswellic acid attenuates titanium particle-induced osteogenic inhibition via activation of the GSK-3beta/beta-catenin signaling pathway. Theranostics. 2019;9(24):7140-55.
20. Wang Y, Yu D, Liu Z, Zhou F, Dai J, Wu B, et al. Exosomes from embryonic mesenchymal stem cells alleviate osteoarthritis through balancing synthesis and degradation of cartilage extracellular matrix. Stem Cell Res Ther. 2017;8(1):189.
21. Trachana V, Mourmoura E, Papathanasiou I, Tsezou A. Understanding the role of chondrocytes in osteoarthritis: utilizing proteomics. Expert Rev Proteomics. 2019;16(3):201-13.
22. Yang Y, Wang Y, Kong Y, Zhang X, Zhang H, Feng X, et al. Moderate Mechanical Stimulation Protects Rats against Osteoarthritis through the Regulation of TRAIL via the NF-kappaB/NLRP3 Pathway. Oxid Med Cell Longev. 2020;2020:6196398.
23. Philpott HT, O'Brien M, McDougall JJ. Attenuation of early phase inflammation by cannabidiol prevents pain and nerve damage in rat osteoarthritis. Pain. 2017;158(12):2442-51.
24. Rahmati M, Nalesso G, Mobasheri A, Mozafari M. Aging and osteoarthritis: Central role of the extracellular matrix. Ageing Res Rev. 2017;40:20-30.
25. Zhou F, Mei J, Han X, Li H, Yang S, Wang M, et al. Kinsenoside attenuates osteoarthritis by repolarizing macrophages through inactivating NF-kappaB/MAPK signaling and protecting chondrocytes. Acta Pharm Sin B. 2019;9(5):973-85.
26. Wu Y, Lin Z, Yan Z, Wang Z, Fu X, Yu K. Sinomenine contributes to the inhibition of the inflammatory response and the improvement of osteoarthritis in mouse-cartilage cells by acting on the Nrf2/HO-1 and NF-kappaB signaling pathways. Int Immunopharmacol. 2019;75:105715.
27. Wang Z, Huang J, Zhou S, Luo F, Xu W, Wang Q, et al. Anemonin attenuates osteoarthritis progression through inhibiting the activation of IL-1beta/NF-kappaB pathway. J Cell Mol Med. 2017;21(12):3231-43.

28. Hu Y, Gui Z, Zhou Y, Xia L, Lin K, Xu Y. Quercetin alleviates rat osteoarthritis by inhibiting inflammation and apoptosis of chondrocytes, modulating synovial macrophages polarization to M2 macrophages. Free Radic Biol Med. 2019;145:146-60.
29. Hu H, Li Y, Xin Z, Zhanga X. Ginkgolide B exerts anti-inflammatory and chondroprotective activity in LPS-induced chondrocytes. Adv Clin Exp Med. 2018;27(7):913-20.
30. Takada Y, Ichikawa H, Badmaev V, Aggarwal BB. Acetyl-11-keto-beta-boswellic acid potentiates apoptosis, inhibits invasion, and abolishes osteoclastogenesis by suppressing NF-kappa B and NF-kappa B-regulated gene expression. J Immunol. 2006;176(5):3127-40.
31. Ding Y, Qiao Y, Wang M, Zhang H, Li L, Zhang Y, et al. Enhanced Neuroprotection of Acetyl-11-Keto-beta-Boswellic Acid (AKBA)-Loaded O-Carboxymethyl Chitosan Nanoparticles Through Antioxidant and Anti-Inflammatory Pathways. Mol Neurobiol. 2016;53(6):3842-53.
32. Sayed AS, Gomaa IEO, Bader M, El Sayed N. Role of 3-Acetyl-11-Keto-Beta-Boswellic Acid in Counteracting LPS-Induced Neuroinflammation via Modulation of miRNA-155. Mol Neurobiol. 2018;55(7):5798-808.
33. Lepetsos P, Papavassiliou KA, Papavassiliou AG. Redox and NF-kappaB signaling in osteoarthritis. Free Radic Biol Med. 2019;132:90-100.
34. Napetschnig J, Wu H. Molecular basis of NF-kappaB signaling. Annu Rev Biophys. 2013;42:443-68.
35. Jimi E, Fei H, Nakatomi C. NF-kappaB Signaling Regulates Physiological and Pathological Chondrogenesis. Int J Mol Sci. 2019;20(24).
36. Herrero-Beaumont G, Perez-Baos S, Sanchez-Pernaute O, Roman-Blas JA, Lamuedra A, Largo R. Targeting chronic innate inflammatory pathways, the main road to prevention of osteoarthritis progression. Biochem Pharmacol. 2019;165:24-32.
37. Catrysse L, van Loo G. Inflammation and the Metabolic Syndrome: The Tissue-Specific Functions of NF-kappaB. Trends Cell Biol. 2017;27(6):417-29.
38. Khan NM, Haseeb A, Ansari MY, Devarapalli P, Haynie S, Haqqi TM. Wogonin, a plant derived small molecule, exerts potent anti-inflammatory and chondroprotective effects through the activation of ROS/ERK/Nrf2 signaling pathways in human Osteoarthritis chondrocytes. Free Radic Biol Med. 2017;106:288-301.
39. Hussain S, Sun M, Min Z, Guo Y, Xu J, Mushtaq N, et al. Down-regulated in OA cartilage, SFMBT2 contributes to NF-kappaB-mediated ECM degradation. J Cell Mol Med. 2018;22(11):5753-8.
40. Luo Z, Zheng B, Jiang B, Xue X, Xue E, Zhou Y. Peiminine inhibits the IL-1beta induced inflammatory response in mouse articular chondrocytes and ameliorates murine osteoarthritis. Food Funct. 2019;10(4):2198-208.
41. Henke JM, Bassler BL. Bacterial social engagements. Trends Cell Biol. 2004;14(11):648-56.
42. Chambers CE, Visser MB, Schwab U, Sokol PA. Identification of N-acylhomoserine lactones in mucopurulent respiratory secretions from cystic fibrosis patients. FEMS Microbiol Lett. 2005;244(2):297-304.

43. Smith RS, Fedyk ER, Springer TA, Mukaida N, Iglewski BH, Phipps RP. IL-8 production in human lung fibroblasts and epithelial cells activated by the Pseudomonas autoinducer N-3-oxododecanoyl homoserine lactone is transcriptionally regulated by NF-kappa B and activator protein-2. J Immunol. 2001;167(1):366-74.

Table

Table 1. The primer sequences

	Primer sequence	
mRNA	Forward(5'-3')	Reverse(3'-5')
IL-1β	GCCCATCCTCTGTGACTCAT	AGGCCACAGGTATTTTGTCG
IL-6	TTGGGAAGGTTACATCAGATC	GGGTTGGTCCATGTCAATTT
TNF-α	GATGGACTCACCAGGTGAG	CTCATGGTGTCCTTTCCAGG
Aggrecan	GAGAAGGAGGTAGTGCTGCTGG	GATGCACAAGGTAATGTCTCGGTA
collagen II	TCCTAAGGGTGCCAATGGTGA	GGACCAACTTTGCCTTGAGGAC
MMP-1	TAGGTGTGGGGTGCCTGATG	GCTCTCTCGATGGCGTTTTCT
MMP-3	CCTCTATGGACCTCCCACAGAATC	GGTGCTGACTGCATCGAAGGACAAA
MMP-13	CTGGCCTGCTGGCTCATGCTT	CCTCAGAAAGAGCAGCATCGATATG
GAPDH	ACTGGCGTCTTCACCACCAT	AAGGCCATGCCAGTGAGCTT

Figures

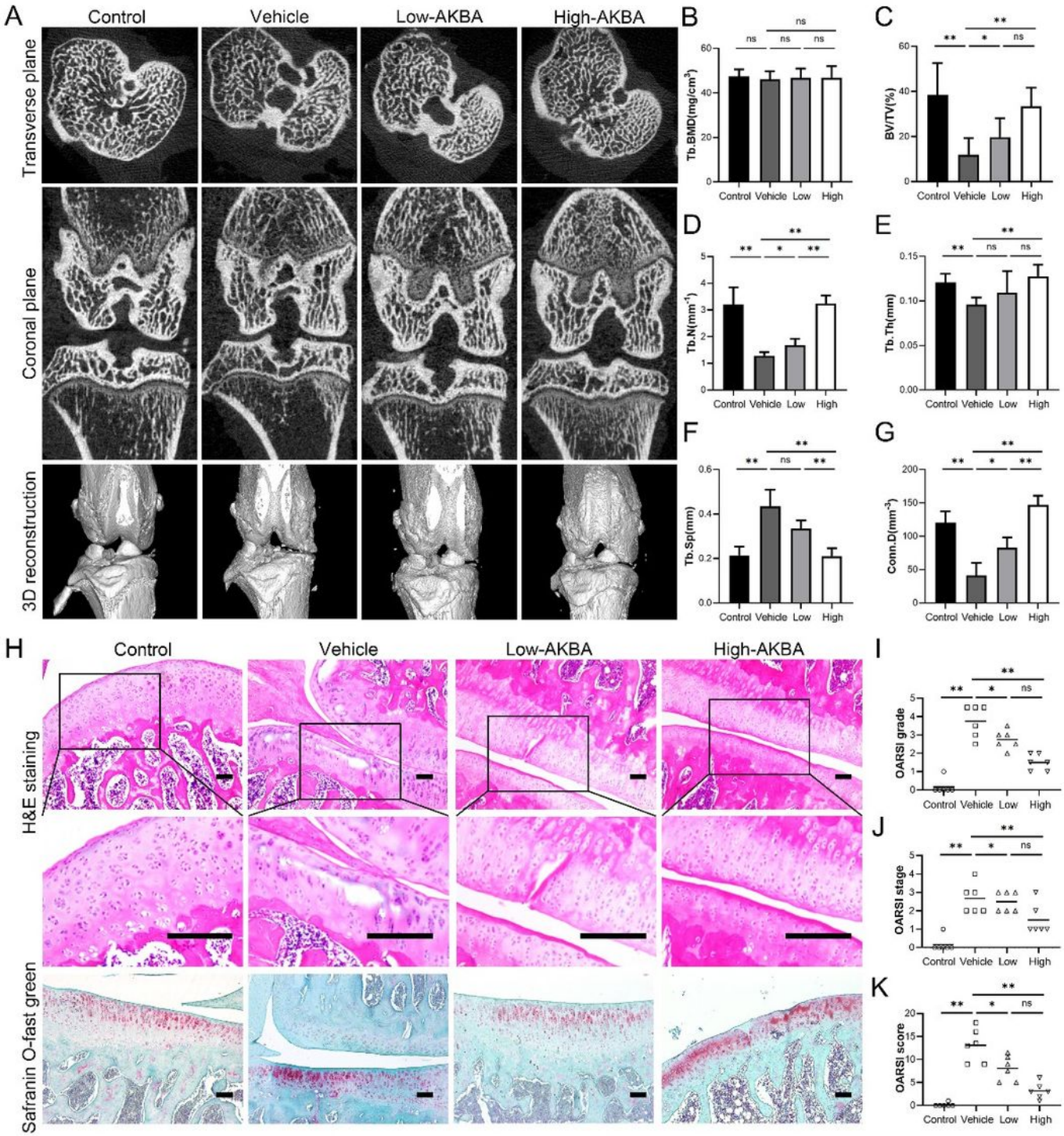

Figure 1

AKBA treatment attenuated surgery-induced bone loss and increased bone mass in a rat Hulth-Telhag model. (a) micro-CT reconstruction images from different experimental groups, (b-g) Bone trabecular bone density (Tb. BMD, mg/cm^3), bone volume fraction (BV/TV, %), number of trabecular bone (Tb. N, mm^{-1}), thickness of trabecular bone (Tb. Th, μm), trabecular bone separation (Tb. Sp, mm), and connection density (Conn. D, mm^{-1}), (h) H&E staining and safranin O-fast green staining, (i-k) OARSI

grade, OARSI stage, and OARSI score. Both low-AKBA (2 mg/kg every other day) group and high-AKBA (8 mg/kg every other day) group received surgery intervention. n=6 per group. Scale bar=100μm. Data are presented as means ± SD. *P<0.05 and **P<0.01, vs. vehicle group.

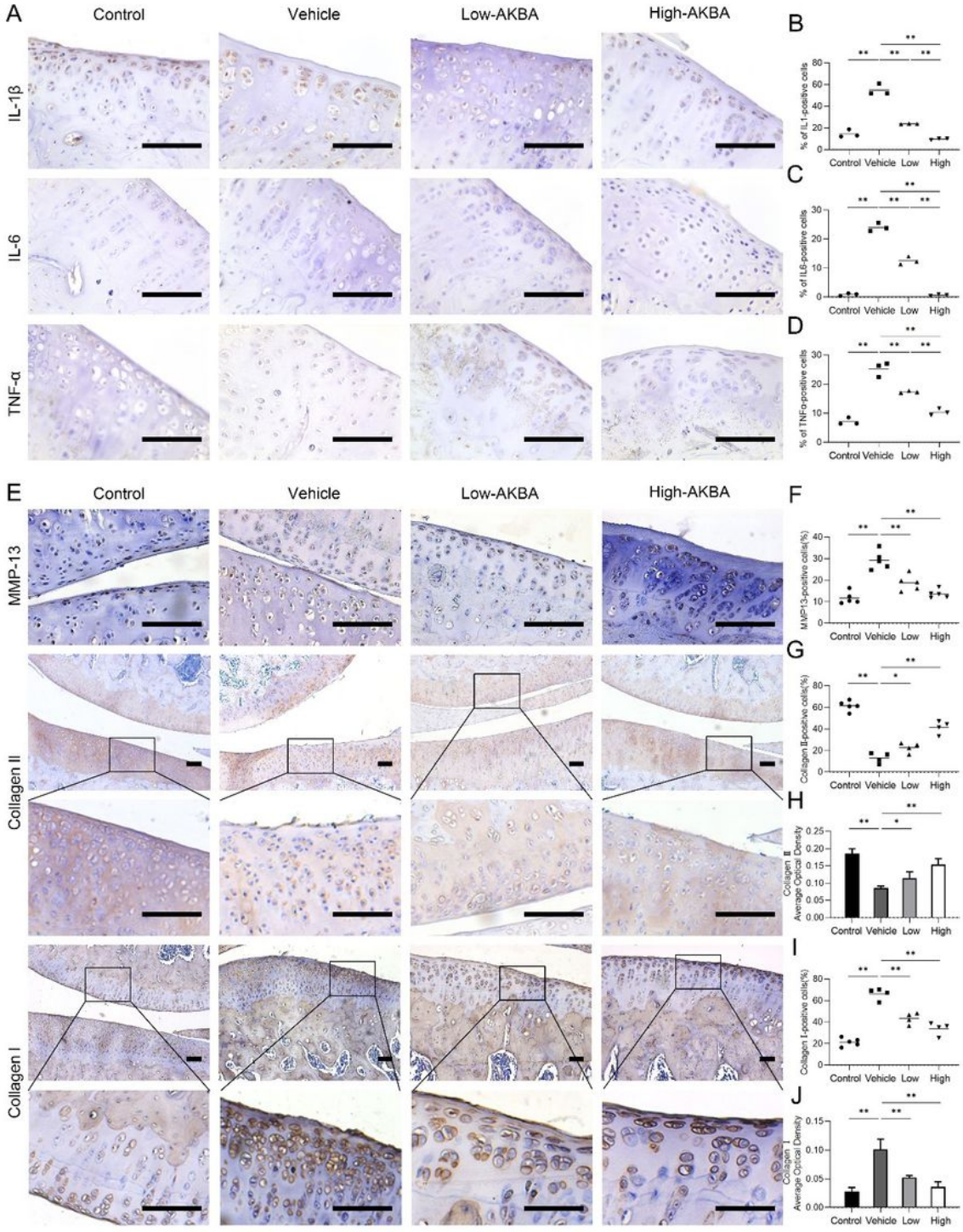

Figure 2

AKBA intervention attenuated inflammation and ECM degradation in a rat Hulth-Telhag OA model. (a) IHC for IL-1β, IL-6, and TNF-α. (b-d) The percentage of cells positive for IL-1β, IL-6, and TNF-α. (e) IHC for MMP-13, col II, and col I. (f, g, and i) The percentage of cells positive for MMP-13, col II, and col I. (h, j) Average optical density for col II and col I. Both low-AKBA (2 mg/kg every other day) group and high-AKBA (8 mg/kg every other day) group received surgery intervention. n=6 per group. Scale bar=100μm. Data are presented as means ± SD. *P<0.05 and **P<0.01, vs. vehicle group.

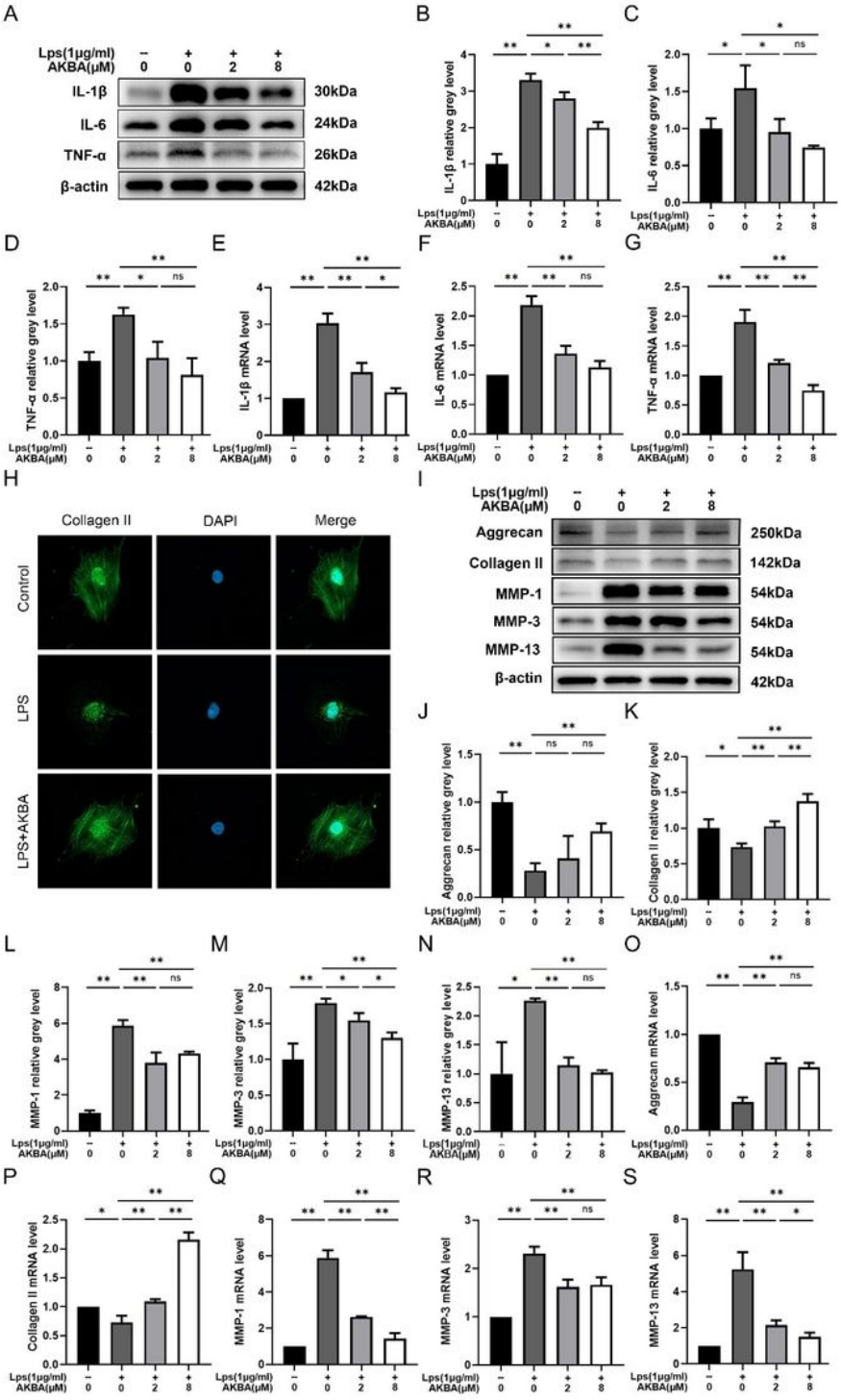

Figure 3

AKBA intervention attenuated inflammation and ECM degradation in LPS-induced rat chondrocytes. (a-d) IL-1β, IL-6, and TNF-α protein expression levels. (e-g) IL-1β, IL-6, and TNF-α mRNA expression levels. (h) Cellular immunofluorescence of col II in chondrocytes. (i-n) Agg, col II, MMP-1, MMP-3, and MMP-13 protein expression levels. (o-s) Agg, col II, MMP-1, MMP-3, and MMP-13 mRNA expression levels. Relative grey levels were quantified using Image J. Both low-AKBA (2 μM) group and high-AKBA (8 μM) group contained 1μg/ml LPS. Dates are presented as means ± SD of six duplicate experiments. *P<0.05, **P<0.01.

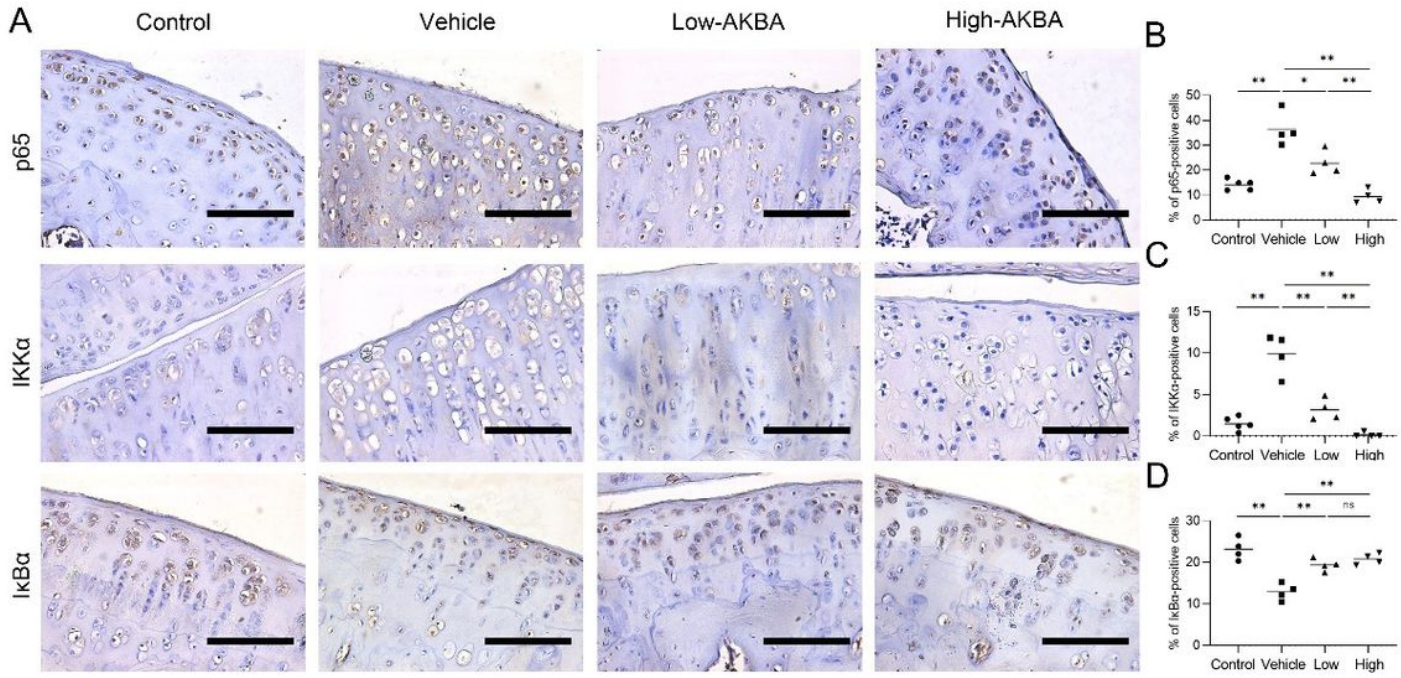

Figure 4

AKBA intervention inhibited the NF-κB signaling pathway in a rat Hulth-Telhag OA model. (a) IHC analysis of the expression of p65, IKKα, and IκBα. (b-d) Quantification of the number of positive cells. Both low-AKBA (2 mg/kg every other day) group and high-AKBA (8 mg/kg every other day) group received surgery intervention. n=6 per group. Scale bar=100μm. Data are presented as means ± SD. *P<0.05, **P<0.01.

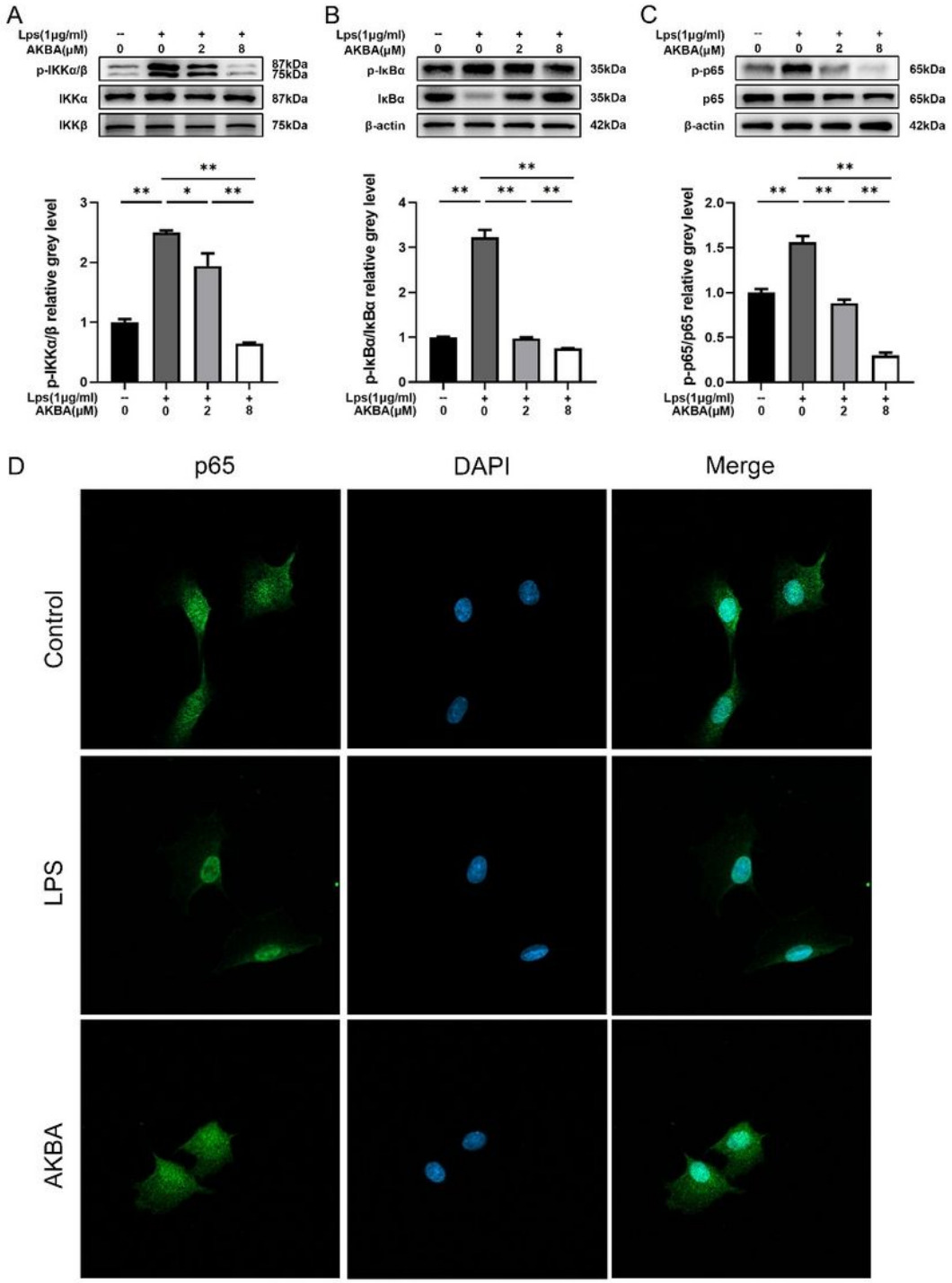

Figure 5

AKBA intervention attenuated NF-κB activation in LPS-induced rat chondrocytes. (a-c) Western blot analysis of expression levels of p-IKK, IKK, p-IκBα, IκBα, p-P65, and P65. The relative grey levels of p-IKK/IKK, p-IκBα/IκBα, and p-P65/P65. (d) Cellular immunofluorescence of p65 in chondrocytes. Relative grey levels were quantified using Image J. Both low-AKBA (2 μM) group and high-AKBA (8 μM) group

contained 1μg/ml LPS. Dates are presented as means ± SD of six duplicate experiments. *P<0.05, **P<0.01.

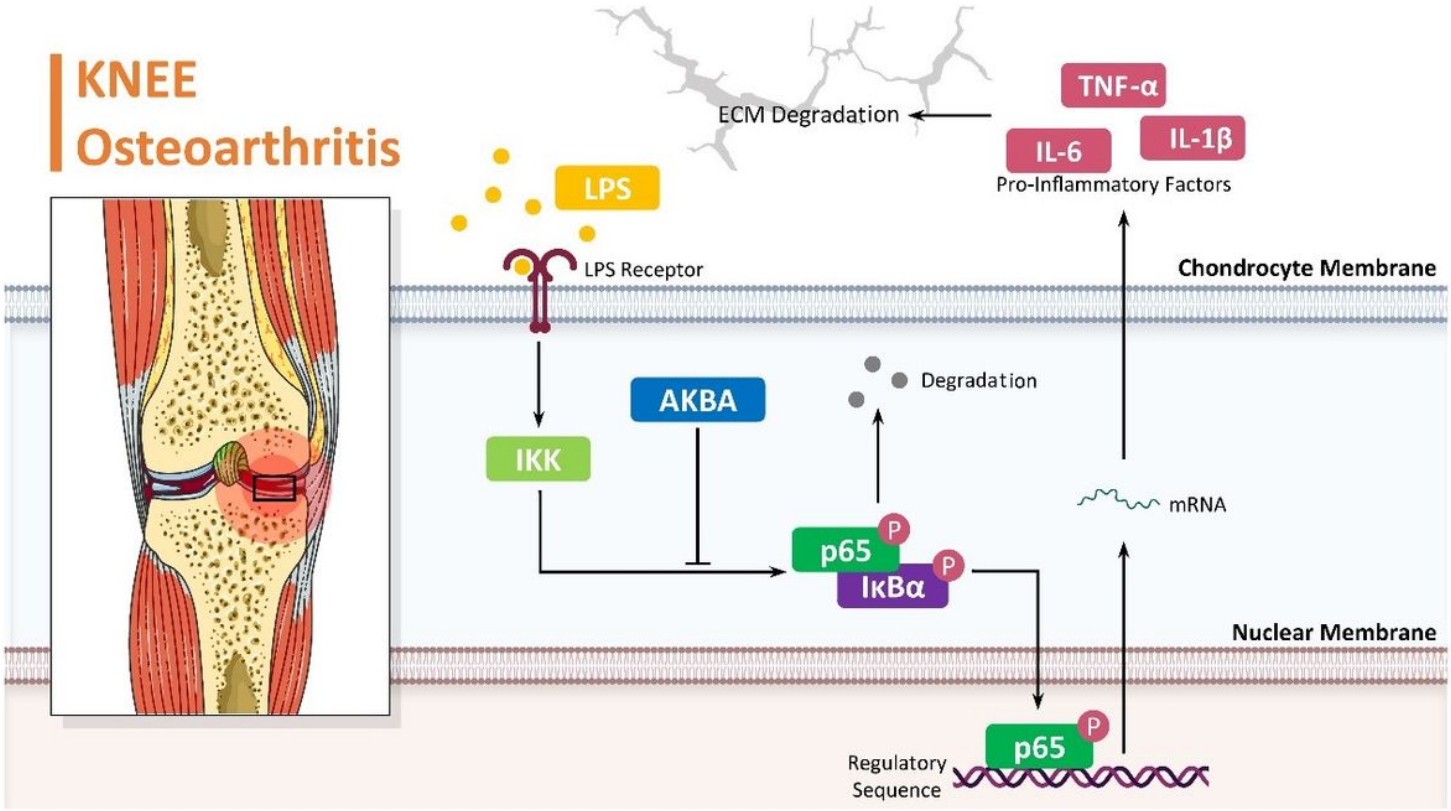

Figure 6

Molecular mechanism of AKBA on LPS-induced rat chondrocytes.

Supplementary Files

This is a list of supplementary files associated with this preprint. Click to download.

- SupplementaryFigures.docx